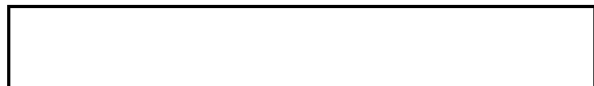


25X1.



Rec'd 26 Apr 72

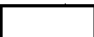
BIBB

HIGH INTENSITY LIGHT SOURCE SYSTEM MODIFICATION EFFORT

STATEMENT OF WORK


0191 DA

Purpose

This modification is proposed by  to bring the performance of the HILS System into conformance with goals established by the customer at a final design review conference held April 24 through 26, 1972. While the HILS System generally meets the requirements of the Design Objectives, several aspects of its operation not previously specified are felt to need further refinement.

25X1

25X1

 will perform the following tasks:1. Tracking Modification

Design, fabricate, assemble, and test modifications to the electronic drive amplifiers to provide more precise tracking of the HILS with the microscope bridge. The dynamic tracking lag experienced during high speed manual bridge operation will be reduced, the goal for this effort will be to maintain the HILS positioned within $\pm 3/8$ inch of the nominal rhomboid position during all normal bridge operations.

Analysis, testing, and subsystem operation will be performed to assure that the present low speed tracking accuracy of $\pm 1/8$ inch will be preserved, and that the existing features of smooth acceleration and controlled response of the HILS assemblies will be maintained.

2. Cooling System

Design, fabricate, assemble and test a modified HILS cooling system. The goal of this effort will be to further reduce the exhaust air sound level and temperature while maintaining the present level of cooling of the HILS and light trays.

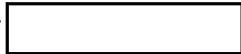
25X1



3. System Testing

Run the system for a period of three weeks in an operational mode to establish reliability of the electronic and mechanical elements prior to delivery. Present to the customer a detailed list of failures and corrective action taken.

4. Delivery and ATP

Provide installation and checkout at the customer's facility, and assist in performance of the final ATP. Services to be provided by 

25X1

5. Schedule

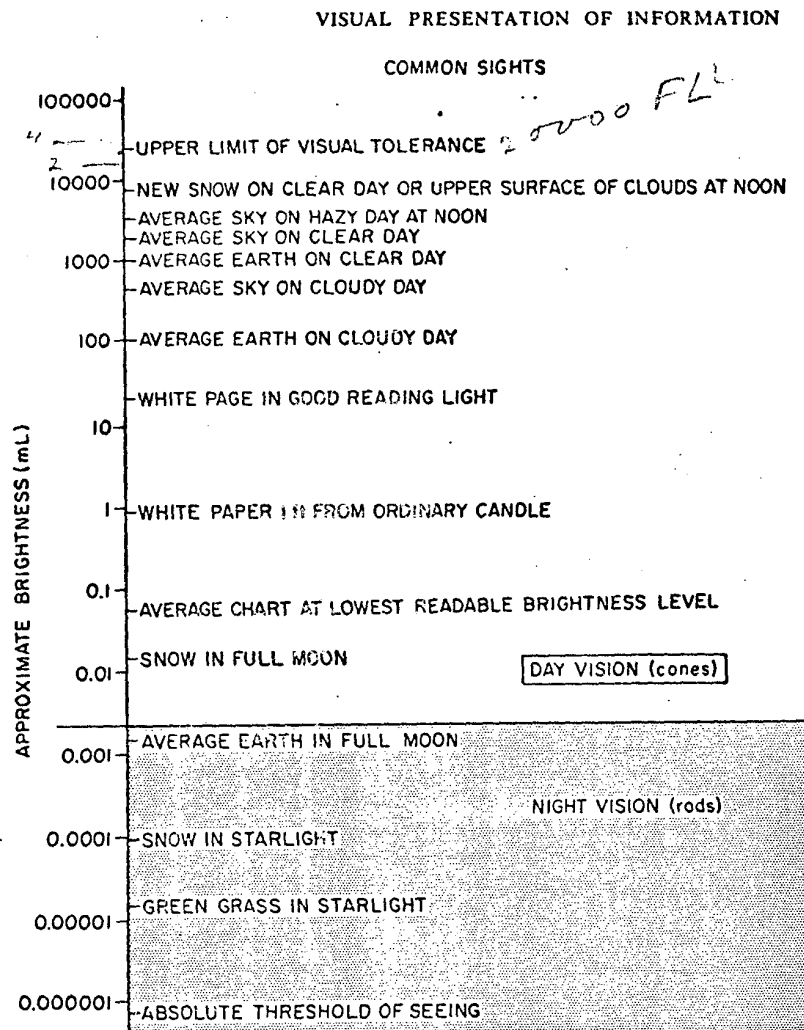
The schedule for the completion of above tasks is six (6) weeks from receipt of approval.

25X1

Approved For Release 2005/02/17 : CIA-RDP78B05171A000400020028-1

Approved For Release 2005/02/17 : CIA-RDP78B05171A000400020028-1

CIBI PA



2-19

and no rods. Because the cones are insensitive to twilight or night conditions, foveal vision is not effective in seeking out dim targets after dark. But, as the angle of view from the fovea is increased, the concentration of rods becomes denser, and night vision is enhanced.

When you want to see something in ordinary daylight, you turn your eyes toward it—you point your fovea toward it—because this is the most sensitive part of the eyes in daylight. At night—when the illumination is below that of about full moonlight—this part of the eye is almost blind, and you cannot see faint targets at night by looking directly at them—you must look slightly away from them.

The curves of Fig. 2-20 (Mandelbaum and Sloan, 1947) show acuity of different parts of the eye at different levels of brightness. Zero on the abscissa scale corresponds to the fovea; the other numbers correspond to different angular positions toward the side away from the nose (temporal angles).

Note from Fig. 2-20 that, at high levels of brightness, the central part of the retina has the best acuity, and that acuity decreases as the temporal angle increases. When the brightness is a little less than 0.04 mL, acuity in the central part of the retina is not as good as acuity about 4 deg away from the fovea. Also, at lower levels of brightness—the equivalent of a dark, moonless night—acuity is

THE BRIGHTNESS PICTURE

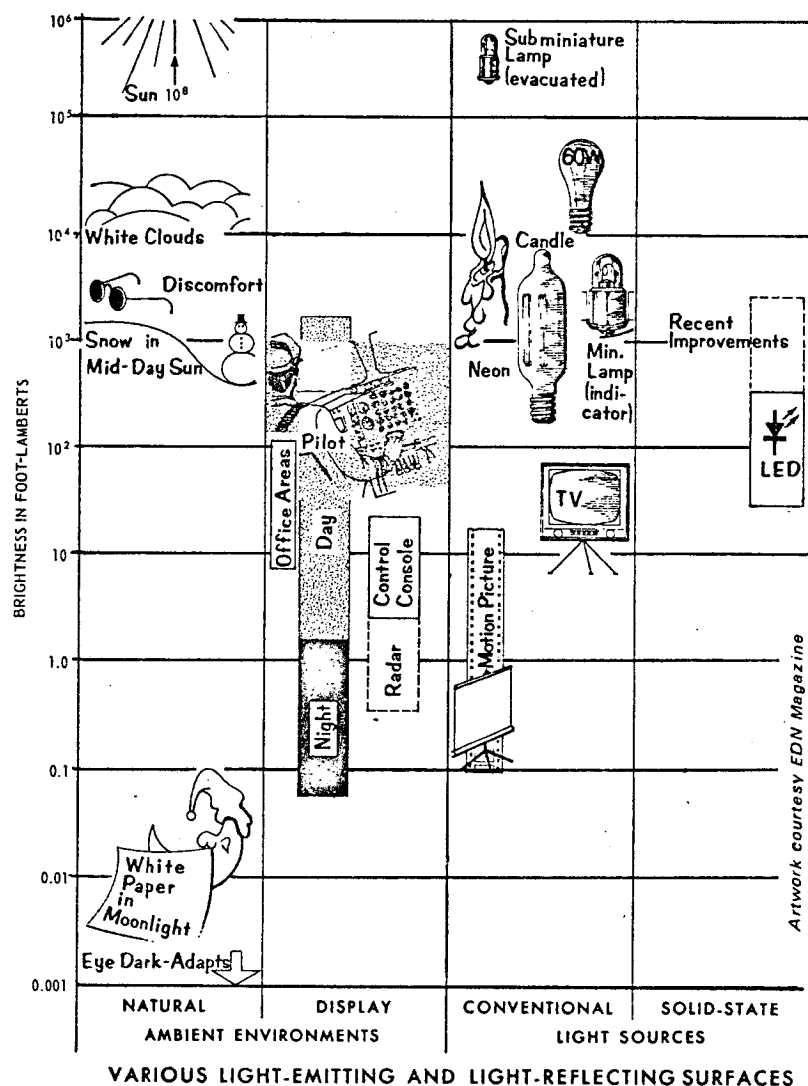
Brightness can be the overriding factor in a decision of whether or not to use solid-state displays. Present LED's don't put out much light. Fortunately, many of the most important man-computer displays don't require much light.

The picturegraph to the right stacks up the brightness levels of various environments against the brightness levels of various light sources. Up is bright; down is dark.

The brightness unit is the foot-lambert (fL), which measures how bright surfaces appear to humans. It is analogous to the decibel, which measures how loud sounds seem. Like human hearing, human vision takes in quite a dynamic range, going from 10^{-6} at which surfaces are too dark to see up to 10^{+5} above which the eye may be harmed.

Most of the surfaces from which we gather visual intelligence have brightnesses in the 1 to 100 fL range. This page probably has a brightness somewhere between 10 and 40 fL. But, in the subdued light of a motion-picture theater or in your auto at night, the screen or dash can transmit intelligible symbols at brightnesses ranging from 0.01 to 5 fL.

LED's, it can be seen, are substantially less bright than most previous light sources. They have surface brightnesses in the 1 to 300 fL range as compared to neons midway between 100 and 1000 and small incandescents going from 1000 to 10,000. Some recent GaAsP LED's are showing brightnesses of 1800 fL but it must be remembered that the light is coming from a very small area.



An Equilibrium Thermal Model for Retinal Injury from Optical Sources

A. M. Clarke, Walter J. Geeraets, and William T. Ham, Jr.

A uniform absorption thermal model is described which allows the calculation of the temperature rise in the retina due to steady state or continuous optical irradiation. Temperature rises of 9-10°C are found to correspond to the production of threshold lesions. For a worst case approximation, a power of 1-2 mW entering the eye and focused onto a 10-μ diam area for 250 msec or longer can be shown as sufficient to cause irreversible damage.

Introduction

The recent advances in the state of the art in the production of continuous laser devices have led to a growing concern over just what level of intensity can be considered hazardous to the eye.^{1,2}

Data on the production of threshold irreversible lesions are available for a wide range of exposure times.¹⁻⁸ Unfortunately, the difficulty in properly observing extremely small lesions (less than 100-μ diam), puts this size range in a very critical region of observation.⁹

Several investigators have proposed models to allow the extrapolation of the presently available data to smaller image diameters where the calculations are made such that the time-temperature history of the various image sizes is the same.⁴⁻¹²

Most of the models proposed to date consider a uniform heat generator, instead of a heat generator function more closely approximating Lambert-Beers absorption. Although the uniform generator choice lends itself to easier computer mapping of the temperature within the absorbing (generating) medium, it fails in the region of small diameter irradiations, as well as for very short exposure times. An error of 30% occurs when the uniform generator is used for the 10-μ diam, steady state case.

The purpose of this presentation is to give a simple steady state thermal model for the retina which, when used with data taken in the laboratories at the Medical College of Virginia and elsewhere, gives values of the temperature rise at the irradiated site which are consistent with measurements and observations on other biological systems and allows the extrapolation of presently available data to the more difficult to measure smaller sizes.

The authors are with the Medical College of Virginia, Richmond, Virginia 23219.

Received 25 July 1968.

The Model

It has been shown¹³⁻¹⁶ that the melanin granules, which are primarily responsible for the absorption of light in the retina, are distributed in such a way as to allow the examination of the absorption properties of the pigment epithelium (P.E.) and choroid separately. If we consider that this distribution is such that these layers each act as a uniform absorber, but with different absorption coefficients, the simple model of Fig. 1 will describe the absorbing media adequately. The uniform absorption, as a consequence of a larger fraction of the total energy being absorbed in the inner sections of the P.E. and choroid results in a lower temperature at the hottest point than uniform generator models of Vos¹⁰ and Hansen *et al.*¹² The power density remaining in the beam as it penetrates the eye is shown in Fig. 2. A uniform beam cross section is assumed for the model in question, as it fits the data presently available. A gaussian cross section will be considered in a subsequent paper.

Putting the model into the steady state heat equation:

$$\nabla^2 T = -A(r, \theta, x)/K,$$

where T = temperature (above ambient); K = thermal conductivity; A = heat generator function = $A(r, \theta, x) = A_0 e^{-\alpha x} = \alpha \sigma_0 e^{-\alpha x}$ ($0 \leq x \leq c$, $0 \leq r \leq b$, $0 \leq \theta \leq 2\pi$) = 0 elsewhere; α = absorption coefficient; σ_0 = surface power density; we obtain, for the axial temperature,

$$T(x_a) = (\alpha \sigma_0 / 2K) e^{-\alpha c} \times \int_0^c e^{\alpha x'} [b^2 + (x - x')^2]^{1/2} - |x - x'| dx'.$$

This can be expanded in a series and integrated term by term, and the ensuing series, with the proper substitution of Legendre polynomials,^{17,18} will allow the computation of off-axial temperatures. However, the results obtained and presented here are for the on-axis case. The numerical integration has been performed

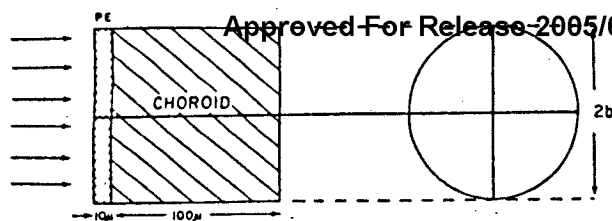


Fig. 1. Cross section of light absorbing medium.

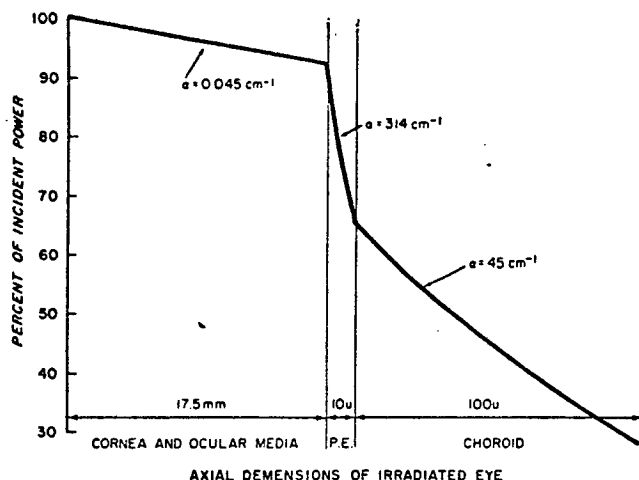


Fig. 2. Intensity profile of the irradiating beam as it passes through the eye.

by a modified trapezoidal rule technique.* The P. E. and choroid were considered separately using thicknesses of $10\ \mu$ and $100\ \mu$, respectively, with absorption coefficients of $314\ \text{cm}^{-1}$ and $45\ \text{cm}^{-1}$. These values represent the average absorption coefficients for the retina and choroid for the spectrum of the high pressure xenon arc as modified by the Schott KG-3 filter used to obtain the data presented in Fig. 3. The absorption coefficients for this integrated spectrum very closely approximate those of the 632.8-nm helium-neon laser wavelength and are obtained using the data of Geeraets and Berry.¹⁶ The temperature map along the axis of the cylinder irradiated was then made by a superposition of the results. The relation of the spatial parameters in the cylinder are shown in Fig. 4.

The tissue cylinders are considered to have the thermal characteristics of water

$$[K = 1.49 \times 10^{-3} (\text{cal/cm sec})^\circ\text{C}],$$

and the choroidal blood flow has been neglected.

Results

Using the machine solution for various radii of interest between $5\ \mu$ and $1000\ \mu$, we obtain values which are given in Table I. These values are for the randomly selected rabbits from chinchilla gray and Dutch strains used in the MCV laboratory, whose ocular spectral

characteristics are discussed in detail by Geeraets and Berry.¹⁶ The radius, temperature rise for a power density of $1\ \text{W/cm}^2$ on the retina, axial position of the hottest point, power density at the retina for a 10°C temperature rise, and the total power entering the eye which will cause a temperature rise of 10°C are given. Figure 3 illustrates the 10°C isotherm (column 4 of Table I plotted against column 1). The choroidal contribution ranges from 50% for a radius of $1000\ \mu$ to 16% for a radius of $10\ \mu$.

Data taken for irreversible threshold lesions in this laboratory are plotted in Fig. 3 and correspond to a temperature rise in the retina of $9\text{--}10^\circ\text{C}$ for exposures

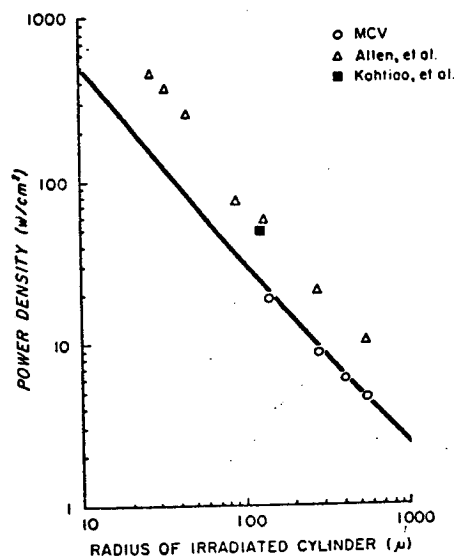


Fig. 3. 10°C temperature rise isotherm.

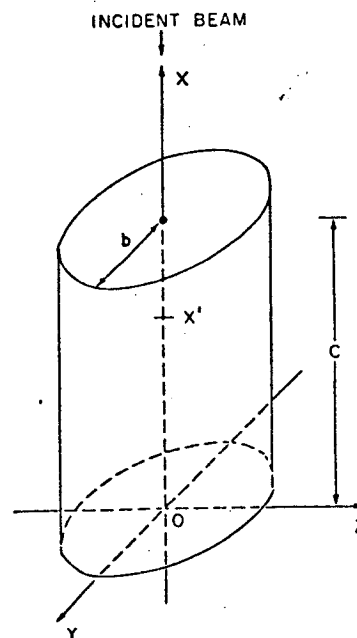


Fig. 4. Relation of the spatial parameters used in the integration.

* This Fortran program, called *Hotspot Check*, is available from the authors.

Table I. Retinal Temperature Rise Due to Optical Irradiation for the Rabbit

Radius (μ)	Temperature rise ^a [$^{\circ}\text{C}/\text{W}/\text{cm}^2$]	Position of hottest point (μ)	Power density at the retina for 10°C temperature rise (W/cm^2)	Power entering eye for 10°C temperature rise (mW)
1000	4.15	10-	2.41	82.3
800	3.30	10-	3.03	66.2
500	2.03	9+	4.93	42.1
400	1.60	9+	6.25	34.1
250	0.968	9	10.3	20.0
200	0.758	9-	13.2	18.0
150	0.550	8+	18.2	14.0
100	0.345	8-	29.0	9.90
75	0.247	7+	40.5	7.78
50	0.152	7-	65.8	5.62
25	0.0648	6	154	3.29
12.5	0.0269	5+	372	1.98
10.0	0.0201	5	498	1.70
5.0	0.0078	5-	1282	1.09

^a Spectral and spatial similarities between the human and rabbit retina make these calculations applicable to the human.

^b As measured at the hottest point.

^c Behind the anterior boundary of the pigment epithelium.

of several minutes. The establishment of equilibrium for exposure durations of this length can be assumed from the trends of the data and calculations (shown in Ham *et al.*, Ref. 5, Figs. 1 and 2). A plot of the data of Allen *et al.*,¹⁹ whose rabbit experiments with a white light source closely parallel those of the MCV laboratory, yields a temperature rise of 20–30°C. The discrepancy is probably due to a difference in the physical characteristics of the light sources used.

Conclusions

Using the model presented, one can take the threshold burn data available for continuous or long time irradiation and, based on the criterion used for the threshold, establish an isotherm for the threshold case of the particular species used as the subject. This isotherm may then be extended to the difficult-to-observe very small lesions, giving values for threshold energies well below the range of sizes of observation which can be conveniently made in the laboratory. Changing absorption parameters from one species to another will allow the calculation of the threshold power needed to produce the irreversible lesions in a second species. Owing to the similarity in the spectral characteristics of the human and rabbit eye, this extrapolation of species is not given here.

The temperature elevation of 9–10°C for threshold burns is realistic but may be slightly on the low side. Equivalent research into skin burns^{20,21} shows that a temperature rise of approximately 15°C is sufficient to cause a blister to appear in 100 sec. This is a more drastic alteration than the criteria used for retinal burns, which would more or less validate the 9–10°C rise found for the data presented.

Finally, using the results presented in Fig. 3, and the procedure described at the first of this section, a worst case condition for thermal damage from a far field light source can be calculated. This is the last

value given in Table I and indicates that a total of 1–2 mW of visible white light or He-Ne laser light entering the eye would be sufficient to cause irreversible damage if focused on a 10- μ worst case diameter area,²² for exposure durations of 250 msec or more. Retinal pigmentation variations between individuals would give a small safety factor to persons with lightly pigmented retinæ, but would lower this value to approximately 1 mW for darker retinæ.

The authors wish to gratefully acknowledge the technical assistance of Eleanor Campbell, and R. C. Williams, H. A. Mueller, R. S. Ruffin, and R. K. Hale.

Support for the research in this paper was provided by contracts with the U.S. Army Medical Research and Development Command, Office of the Surgeon General, and the Defense Atomic Support Agency, Department of Defense, Washington, D. C.

References

1. W. T. Ham, Jr., R. C. Williams, W. J. Geeraets, R. S. Ruffin, H. A. Mueller, *Acta Ophthalmol. Suppl.* 76, 60 (1963).
2. W. T. Ham, Jr., *et al.*, *Acta Ophthalmol.* 43, 390 (1965).
3. W. T. Ham, Jr., *et al.*, "Ocular Effects of Laser Radiation, Part I," DASA Rep. 1574, 1964.
4. W. J. Geeraets *et al.*, *Federation Proc. Suppl.* 14, 24, No. 1, Part III (Jan.-Feb. 1965).
5. W. T. Ham, Jr., R. C. Williams, H. A. Mueller, D. Guerry, III, A. M. Clarke, and W. J. Geeraets, *Trans. N. Y. Acad. Sci.* (2) 28, 517 (1966).
6. W. T. Ham, Jr., in *Proceedings of the First Conference on Laser Safety*, G. W. Flint, Ed. (Martin Company, Orlando, Florida, 1966).
7. A. Kohtiao, I. Resnick, J. Newton, and H. Schwell, *Amer. J. Ophthalmol.* 62, 644 (1966).
8. A. Kohtiao, J. Newton, H. Schwell, and I. Resnick, *Ann. N. Y. Acad. Sci.* 122, 571 (1965).
9. A. E. Jones, D. D. Fairchild, and P. Spyropoulos, "Laser Radiation Effects on the Morphology and Function of Ocular Tissue," Second Annual Rep. DADA-17-67-C-0019 (1968).

10. J. J. Vos, *Bull. Math. Biophys.* **24**, 115 (1962).
11. J. J. Vos, Digital Computations of Temperature in Retinal Burn Problems, Institute for Perception, RVO-TNO, Rep. IZF 1965016, Soesterberg, The Netherlands (1963).
12. W. P. Hansen, L. Feigen, and S. Fine, *Appl. Opt.* **6**, 1973 (1967).
13. W. J. Geeraets, R. C. Williams, G. Chan, W. T. Ham, Jr., D. Guerry, III, and F. H. Schmidt, *Arch. Ophthalmol.* **64**, 606 (1960).
14. W. J. Geeraets, R. C. Williams, G. Chan, W. T. Ham, Jr., D. Guerry, III, and F. H. Schmidt, *Invest. Ophthalmol.* **1**, 340 (1962).
15. W. J. Geeraets *et al.*, *Arch. Ophthalmol.* **69**, 612 (1963).
16. W. J. Geeraets and E. R. Berry, *Amer. J. Ophthalmol.* **66**, 15 (1968).
17. D. L. Ridgeway, to be published.
18. W. R. Smythe, *Static and Dynamic Electricity* (McGraw-Hill Book Company, Inc., New York, 1950), Sec. 5.16, p. 139.
19. R. G. Allen, Jr., *et al.*, "Research on Ocular Effects Produced by Thermal Radiation," Final Rep. AF41(609)-3099 (1967).
20. W. L. Derksen, T. I. Monahan, and G. P. Delhery in *Temperature: Its Measurement and Control in Science and Industry*, J. D. Hardy, Ed. (Reinhold Publishing Corporation, New York, 1963), Vol. 3, Pt. 3, p. 171 ff.
21. F. C. Henriques, Jr., *Arch. Pathol.* **43**, 489 (1947).
22. G. Westhimer and F. W. Campbell, *J. Opt. Soc. Amer.* **52**, 1040 (1962).

Imperial College of Science and Technology
APPLIED OPTICS SECTION

SUMMER SCHOOL
ON
APPLIED OPTICS

for nonspecialists

in optics

9-20 June 1969

The course will be given by various members of the staff of the Applied Optics Section: R. F. Edgar, M. J. Kidger, K. H. Ruddock, R. W. Smith, W. T. Welford, W. D. Wright and C. G. Wynne.

This is an introductory course of about thirty-six lectures, intended for scientists and engineers who have had little or no specialised training in applied optics. Its emphasis will be on basic ideas rather than the detailed development of formulae. The lectures have been revised as a result of experience gained from previous summer schools. Lecture notes will be circulated in advance. Topics to be covered will include paraxial optics, aberrations, coherent and incoherent image formation, design and testing of optical systems, visual perception, photometry, visible and infrared sources and detectors.

The course fee is £35.0.0.

Further details and application forms may be obtained from

The Registrar
Imperial College,
London S.W.7., England

MATCHING AN IMAGE DISPLAY TO A HUMAN OBSERVER

Donald C. Winter
Avco Electronics Division*
Cincinnati, Ohio

The characteristics of the human eye are well known, and Modulation Transfer Functions are old hat, but rarely are these two knowledges combined to form an effective predictive tool for the system designer. Here's one good way it can be done.

The most common ultimate detector for an E-O imaging system is the human eyeball. Image intensifiers may be cascaded into TV camera tubes; scanners may couple to elemental or arrayed detectors; but the final image detection and interpretation usually relies on the old fashioned human eye. Thus, many engineering decisions on the system must be predicted on the characteristics of this ancient device. Of course, the designer's most powerful tool for E-O systems analysis is the Modulation Transfer Function (MTF). Unfortunately, MTF data for the eye can not be obtained without intercepting the signal from eye to brain, but mathematical services depicting the detection threshold of the eye as a function of scene brightness, target contrast and angular size, and observation time can and have been prepared for rudimentary targets by a number of researchers.¹

Combined with MTF curves for the rest of the system, these detection curves can form the basis of a field-of-view vs resolution trade-off, or can be used to predict system performance under a specific set of conditions involving a simple scene.

*Now with Electro-Optical Systems, Pasadena, CA

This article discusses how the output of an imaging system, measured by its MTF, can be matched to the observing abilities of the human observer to improve performance of the display/operator system; reviews development of the MTF for an imaging system other than the eye; notes basic characteristics of human observations; deals with the problem of observing a moving field of view (as in a system for use in a high speed aircraft); measures performance of the human observer in viewing the displayed image with emphasis on discernibility of small targets; and uses that measurement to derive the MTF required for the remainder of the imaging system for best human observing.

The Modulation Transfer Function

The response of an imaging system to a periodic object was developed in 1946 by Duffieux,² working with sinusoidal objects in France, and independently by Schade,³ working with square wave objects in the United States. The relations between the resulting sine wave and square wave responses were shown by Coltman⁴ and by Shack,⁵ in two of the earliest papers on the characteristics of a general imaging system.

The term "Modulation Transfer Function" was adopted in 1961 by the International Committee on Optics.⁶ The Modulation Transfer Function (MTF) is the magnitude of the spatial sine wave response of an optical or electro-optical system. The spatial sine wave response is the ratio of the Fourier transforms of the spatial characteristics of the image and object, in an exact analog of the transfer function used in communication theory.

The spatial characteristics of a sine-wave or square wave object are specified by its spatial frequency (the reciprocal of line-pair width), and by its modulation M (equivalent to the Michelson visibility)⁷:

$$M = \frac{L_{\max} - L_{\min}}{L_{\max} + L_{\min}}$$

Thus the MTF of an imaging system is the ratio of the modulation of the image to the modulation of the object, point by point over a spatial frequency range from zero to some maximum.

Since a sinusoidal input to a linear system always results in a sinusoidal output, the output of one imaging component can be used directly as the input to the next, and the overall MTF of an imaging system is simply the convolution of the MTF's of the

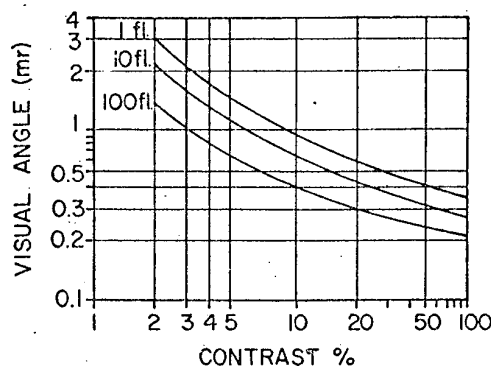


Fig. 1. Visual acuity as a function of contrast for different background luminosities.

individual components, be they optical or electrical.

The application of the MTF to the problem of imaging a small object in a relatively large field (as in aerial reconnaissance) has been described by Kelly⁸ along with the effects of placing two or three small targets close together, also discussed by Perin.⁹ These small targets must be considered as short-duration wideband inputs, rather than long-duration high frequency inputs to the system.

The Human Observer

In an imaging system intended for human observation, the response characteristics of the human visual system must be included in the performance specification. The sine wave response characteristics of the visual system have been investigated by Lowry and DePalma,¹⁰ and data on the discernibility of small targets are given in Luxenberg and Kuehn¹¹ (p. 149). The small target used is the bright bar in a Landolt-ring placed in an array of complete circles. The actual target is, thus, a single narrow bright line.

Lowry and DePalma use a "contrast sensitivity," which is the same as the target modulation M, while the contrast used

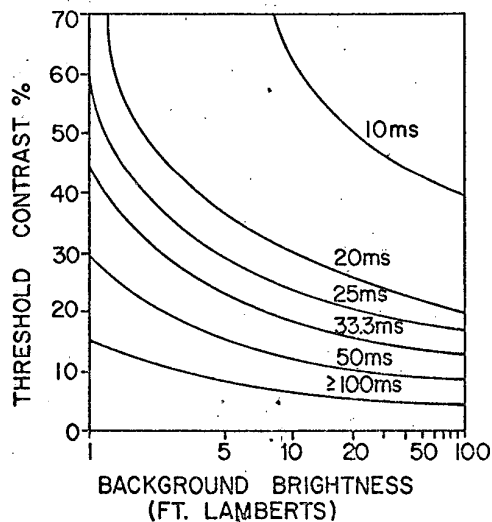


Fig. 2. Threshold contrast versus background brightness at various exposure times.

... brightness difference needed for discernability increases as background gets brighter.

in the small target data is

$$C = \frac{L_T - L_B}{L_B}$$

where: L_T is the target luminance, and L_B is the background luminance." (Luxenberg & Kuehn, p. 106).

The minimum contrast at which the bright line can be detected is called the threshold contrast. These two sets of data cannot be directly compared. The relations between contrast and modulation are:

$$C = \frac{2M}{1-M}; M = \frac{C}{2+C},$$

if the bright line target is compared with one line in the bar chart target.

Even if these conversions are used, a direct comparison proves to be very difficult since Lowry and DePalma data is taken at constant average brightness,

$$\frac{L_{\max} + L_{\min}}{2},$$

whereas the small target data is for constant background brightness. Only for small values of C are these equivalent.

Since small targets, consisting of perhaps two or three bright lines, rather than extended bar charts, are of major interest when considering the most difficult detection situations for an electro-optical imaging system, only the Luxenberg and Kuehn data will be considered further. Samples curves from this data, showing contrast versus visual angle at the eye for various background luminances, are given in Fig. 1. These curves show that the contrast which a target must have, before it can be discerned against the background,

decreases with increasing target size and with increasing background luminance. This means that larger targets can be seen at a smaller contrast. However, although the necessary contrast decreases with increasing background luminance, the brightness difference needed for discernability actually increases as the background gets brighter. The effect this has on the "shades of grey" obtainable on a CRT display will be discussed later in this article.

Integration Effects of the Eye

The fovea of the eye integrates all the radiation it receives at each point within a time interval of about 0.1 sec. For images which are present for a shorter "exposure time" than this integration time, more contrast is needed to achieve the same discernibility. By the Bunsen-Roscoe law,¹² the visual response for short time signals can be characterized by the integral of the luminance taken over 0.1 sec. Thus, the product of exposure time and "threshold" contrast, when the exposure time is less than 0.1 sec., is a constant for a given point on any curve in Fig. 1.

Effects of Moving Images

In its original formulation, the Bunsen-Roscoe law applied only to stationary stimuli of short duration. For consideration of moving images the discernibility of a continuous stimulus moving across the retina must be determined.

Morris¹³ quoted Duntley as saying that: "The effective duration of the target stimulus is the time interval required for the image of the object to pass over point on the retina of the eye if the eye is held steady." Morris also considered some later experimental data and concluded that "Ground targets moving with respect to the line-of-sight can be equated to targets flashed into the center of the field for a single brief exposure, equal in duration to the time required for the target to move across a point on the retina." Thus the exposure time presented by a particular target

can be considered as the length of time the target remains imaged on any one point of the retina. When there is relative motion between the displayed target and the eye, the exposure time is determined by the angular rate of motion and the target's visual angle in the direction of motion as:

$$\text{Exposure time, } t_e = \frac{\text{target angular size}}{\text{angular rate}}$$

When this expression is used for exposure time, the Bunsen-Roscoe law can be assumed to apply equally for the case of stationary flashing sources and moving continuous sources.

Exposure Time and Discernible Contrast

Examples of curves showing the variation of threshold contrast with brightness and exposure time are given in Fig. 2. The curves are obtained from Fig. 1 by using the Bunsen-Roscoe law. If the threshold contrast for a stationary target is 10%, say, then the threshold contrast for an exposure time of 50 ms is 20%, for 25ms it is 40%, for 20 ms 50%, and so on. Such curves show, for example, that a target subtending 0.4 mr at the eye, with an exposure time of 50 ms, would need to be 200% brighter than a background of brightness 20 fL (that is, the target brightness would be 60 fL) in order to be discernible to the eye. A target subtending 2.0 mr, however, would need to be only 2.2% brighter (20.44 fL); with the same exposure time to be discernible against the same background. These curves can be used to determine the minimum discernible brightness difference on the display, for a given target size, exposure time, and background brightness, and the approximate total number of such brightness steps available in a displayed image.

Starting from the "black" level on the display, the threshold contrast determines the minimum discernible brightness above this. Then, the next brightness step (shade-of-grey) is obtained by applying

the threshold brightness for the old level as background for the new one. This procedure can be repeated until the maximum obtainable display brightness is reached. The total number of such steps for a particular target size and exposure time is known as the "number of grey steps" in the image. This term has been the source of much confusion in the past, and in particular the number for one special case has gained wide acceptance as a definition of the term. A sample curve showing the variation of discernible brightness step with the background brightness on the display, together with the total number of steps in each case is shown in Fig. 3. The total number of steps is a function of target size and exposure time for a particular display design. The curve shows that the necessary increase in brightness for a target to be visible on a bright part of the display is much greater than for the same target to be visible on a dark part of the display. The curves also show that the effect of reducing the contrast ratio between the maximum and minimum brightness levels on the display, due to such factors as ambient illumination, is to eliminate the part of the curve where most of the brightness steps occur, since the minimum brightness level is increased while the maximum remains unchanged. Then, since more steps occur in the low brightness portion of the curve, a small reduction in the overall contrast ratio will cause a large reduction in the total number of steps.

Required MTF for Target Detection

The curves of threshold contrast versus brightness given in Fig. 2 can be used to determine the MTF required of an imaging system prior to the display in order for targets subtending a particular visual angle to be discerned in the display.

A system with limited bandwidth will distort a rectangular input pulse into a pulse having a $\frac{\sin x}{x}$ shape^{5,9}. Then the targets appearing on the display have a

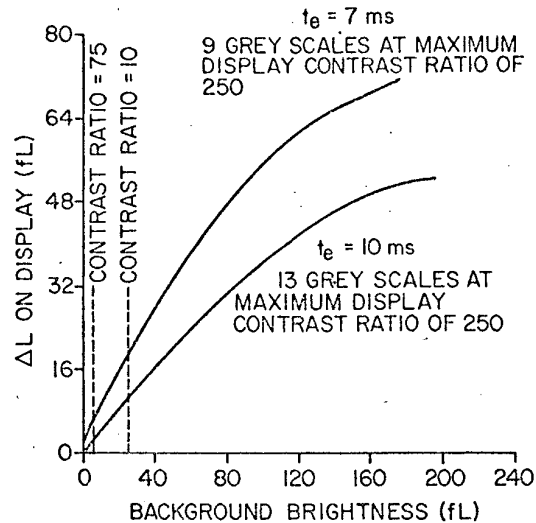


Fig. 3. Discernible brightness difference on display versus background brightness.

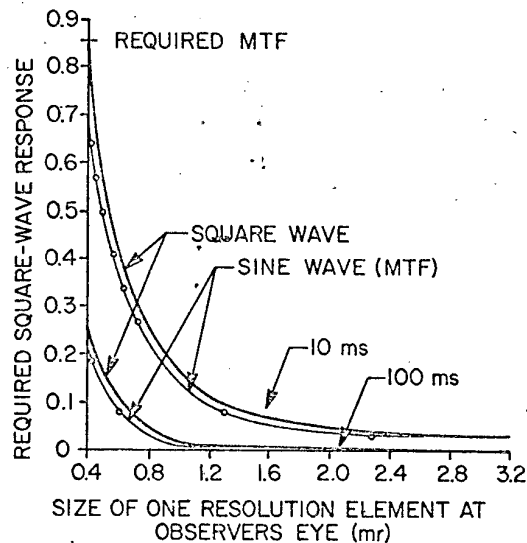


Fig. 4. Required imaging system response.

The square wave response can be easily converted into required MTF by . . .

spatial brightness distribution following the central peak of this wave shape. The effect of bringing two such targets into close proximity, with a separation equivalent to the width of the undistorted targets, is to approximate to reasonable accuracy the response to a square wave input to the system.⁹ The modulation M of this square wave response is obtained by considering the peak of each pulse to be L_{\max} , and the dip in between the pulses as L_{\min} . In order to be easily usable in system design, this square wave response can be converted to the required system MTF by following the method given by Coltman⁴ for conversion to sine wave response.

The curves of Fig. 2 are converted to square wave response curves by applying the conversion between contrast and modulation given in the discussion of integration effects on the eye, and assuming that modulation of the input to be unity. Example curves of the required square wave responses for target detection are given in Fig. 4 for a range of target sizes, one value of background brightness and two exposure times. The same curves converted to show required MTF for target detection are also shown. These curves show, for instance, that in order for a target subtending 0.8 mr at the observer's eye to be discerned against a background of 10 fL, if it is exposed for 10 ms, the imaging system must have an MTF of at least 22% at a spatial frequency of 625 cycles/radian, but in order for a 2.0 mr target to be seen under the same conditions, the system MTF at 250 cycles/radian would need to be only 5.5%. These spatial fre-

quencies are those seen by the observer viewing the display, and will not in general be the same as the spatial frequencies in object space. To obtain the latter the system magnification would have to be taken into account.

Use of the Required MTF Data

The curves of required MTF versus target size at the eye can be used to determine the best compromise between the imaging system magnification from the sensor to the display, and the scanner field-of-view which can be usefully presented to the observer. The eye response curves are valid only over a limited field-of-view at the eyes, which for most purposes is the angle occupied by the fovea (within the circle of rods), which is $\pm 10^\circ$ in azimuth from the visual axis, and $\pm 7.5^\circ$ in elevation. Thus the useful sensor field-of-view is limited to that which, when displayed, occupies 20° azimuth \times 15° elevation at the observer's eyes. As the system magnification increases, the usable sensor field-of-view decreases and thus some compromise magnification giving just sufficient target discernibility must be used.

The determination of the just sufficient magnification is easily accomplished using the required MTF curves. In order to take account of the worst case, the curve for the brightness level corresponding to display black level should be used. The initial value of system magnification is chosen such that one sensor resolution element occupies the minimum usable visual angle at the eye. For example, consider a system on which this method has been used in a theoretical study. For this system the initial magnification is 8. The system field-of-view corresponding to this magnification is $20^\circ/8 = 2.5^\circ$ wide. The system MTF for such a system has been calculated in a theoretical study as 40%. This is then compared with the required value of 75% from Fig. 4. The system MTF is evidently not high enough. The magnification is then increased to 9.6 (corresponding to a field-of-view of

2.0°), and the system MTF for the revised system was calculated as 39%. The required MTF for this magnification is 52%. Again magnification is increased to 11.2 ($\text{FOV} = 1.8^\circ$) and the MTF for this case was found to be 38%, compared with a required MTF of 39%. Evidently, the next increase will be sufficient. At a magnification of 12.8 ($\text{FOV} = 1.6^\circ$) the system MTF was found to be 37% and the required MTF is only 32%. Thus, at this magnification, the minimum sized targets on the display can be discerned by the eye. The magnification is now at a sufficient value for a good compromise between target discernibility and system field-of-view.

This procedure should prove useful in matching the performance of any imaging system to the requirements of the human observer. \square

REFERENCES

1. Campbell, F. W., Proc. of IEEE, 56, 1009 (1968).
2. Duffieux, P. M., *L'Integrale de Fourier et ses Applications a l'Optique*, Besancon, Paris, 1946.
3. Schade, O. H., RCA Rev. 9, 246 (1949).
4. Coltman, J. W., J. Opt. Soc. Am. 44, 468 (1954).
5. Shack, R. V., J. Res. N.B.S. 56, 245 (1956).
6. Recommendation on Nomenclature by ICO Subcommittee for Image Evaluation, Opt. Acta. 8, 359 (1961).
7. Dow Smith, F., Appl. Opt. 2, 335 (1963).
8. Kelly, D. H., Appl. Opt. 4, 435 (1965).
9. Perrin, F. H., J. SMPTE 69, 239 (1960).
10. Lowry & DePalma, J. Opt. Soc. Am. 52, 328 (1962).
11. Luxenberg & Kuehn, *Display Systems Engineering*, McGraw-Hill, 1968.
12. Long, G. E., J. Opt. Soc. Am. 41, 743 (1951).
13. Morris, A., *Predicting the Detection Range of a Target in a Moving Field-of-View*, US Navy Electronics Laboratory, San Diego, Calif. (1959).

Author Donald C. Winter received his B.S. in Electronics from Southampton University in England in 1965 and an M.S. in Electrical Engineering from the University of Cincinnati. In 1961 he joined the Hawker Siddeley Aviation Company where he conducted mission analysis of weapons and avionics systems. In 1966 he joined Avco Electronics Division having responsibility for systems analysis of forward looking infrared systems. Mr. Winter is presently with Electro-Optical Systems, A Xerox Company, in Pasadena, California.